



**AIAA 98-2575**

**Multi-Component Diffusion with  
Application To Computational  
Aerothermodynamics**

Kenneth Sutton and Peter A. Gnoffo  
NASA Langley Research Center  
Hampton, VA 23681-0001

**7th AIAA/ASME Joint Thermophysics  
and Heat Transfer Conference**  
June 15-18, 1998 / Albuquerque, NM

MULTI-COMPONENT DIFFUSION WITH APPLICATION TO COMPUTATIONAL  
AEROTHERMODYNAMICS

Kenneth Sutton\* and Peter A. Gnoffo\*  
NASA Langley Research Center  
Hampton, VA 23681-0001

Abstract

The accuracy and complexity of solving multi-component gaseous diffusion using the detailed multi-component equations, the Stefan-Maxwell equations, and two commonly used approximate equations have been examined in a two part study. Part I examined the equations in a basic study with specified inputs in which the results are applicable for many applications. Part II addressed the application of the equations in the Langley Aerothermodynamic Upwind Relaxation Algorithm (LAURA) computational code for high-speed entries in Earth's atmosphere. The results showed that the presented iterative scheme for solving the Stefan-Maxwell equations is an accurate and effective method as compared with solutions of the detailed equations. In general, good accuracy with the approximate equations cannot be guaranteed for a species or all species in a multi-component mixture. "Corrected" forms of the approximate equations that ensured the diffusion mass fluxes sum to zero, as required, were more accurate than the uncorrected forms. Good accuracy, as compared with the Stefan-Maxwell results, were obtained with the "corrected" approximate equations in defining the heating rates for the three Earth entries considered in Part II.

Nomenclature

$c_i$	mass fraction of species $i$
$D_{ij}$	multi-component diffusion coefficient, $m^2/s$
$\mathcal{D}_{ij}$	binary diffusion coefficient, $m^2/s$

\*Senior Research Engineer, Associate Fellow AIAA

Copyright © 1998 by the American Institute of Aeronautics and Astronautics, Inc. No copyright is asserted in the United States under Title 17, U.S. Code. The U.S. Government has a royalty-free license to exercise all rights under the copyright claimed herein for governmental purposes. All other rights are reserved by the copyright owner.

$D_{im}$	effective diffusion coefficient, $m^2/s$
$F_{ij}$	elements of matrix $\mathbf{F}$ defined by Eq. 7
$i, j$	index on species
$J_i$	diffusion mass flux of species $i$ , $kg/m^2-s$
$M$	molecular weight of mixture, $kg/mole$
$M_i$	molecular weight of species $i$ , $kg/mole$
$n$	total number of species present
$q$	convective heating rate, $W/cm^2$
$r$	local body radius, $m$
$T$	temperature, $K$
$x_i$	mole fraction of species $i$
$\rho$	density, $kg/m^3$
$z$	distance through shock layer, $m$
$\Omega_{ij}$	collision cross section for mass diffusion, $m^2$

Introduction

Accurate knowledge of the diffusion of species in multi-component gas mixtures is important in many engineering applications. Of primary interest in the present study is the impact of multi-component diffusion on the high-velocity flowfield surrounding planetary and Earth entry vehicles. These flowfields contain a highly reactive gas mixture in which the multi-component diffusion of species can significantly alter the local chemical state; and, the accurate prediction of the surface heat transfer is dependent on the species diffusion mass flux at the surface. Computational Fluid Dynamics (CFD) methods are used to solve the complex flowfield over entry vehicles.

Even with today's computers, the multi-component diffusion is often solved with approximate methods due to the large time and storage requirements associated with the detailed multi-component equations. The solution of the detailed equations involve solving determinants that can be quite large in number and size as the number of species increase.

The present paper will report on a study that examines the accuracy and complexity of solving multi-component diffusion including the detailed multi-component equations<sup>1,2</sup>, the Stefan-Maxwell equations<sup>1,3</sup>, and two commonly used approximate relations<sup>4</sup> cast in the formulation of Fick's law for binary diffusion. The study is composed of two parts. In Part I a basic study was conducted that examined the equations in a general manner with specified inputs. The results from this part can be useful and applied to any application for gaseous diffusion. Part II addresses the application of the Stefan-Maxwell equations and the approximate equations in the LAURA (Langley Aerothermodynamic Upwind Relaxation Algorithm) code for entries in Earth's atmosphere. LAURA is a powerful CFD code<sup>5</sup> that solves the Navier-Stokes equations for high-temperature, finite-rate chemistry, supersonic and hypersonic flows over three-dimensional entry vehicles, and has been used in numerous planetary and Earth entry studies.

### Equations

A brief description and comments on the equations of the diffusion mass fluxes and diffusion coefficients used in the present study are given in this section. The equations are for the detailed multi-component equations, the Stefan-Maxwell equations, and the approximate multi-component equations with the binary diffusion equations given for comparison. Some of the equations are written differently than normally presented in the literature. This is done to present a consistent form between the various equations and to highlight certain terms. Also, the gradients of mole fraction and mass fraction are both used as the driving potential and may be referred to as mole gradient and mass gradient, respectively.

#### Binary Diffusion Coefficient

The binary diffusion coefficients<sup>2,3</sup> are used in all the formulations and are given by

$$\rho \mathcal{D}_{ij} = 7.1613 \times 10^{-25} \frac{M \left[ T \left( \frac{1}{M_i} + \frac{1}{M_j} \right) \right]^{1/2}}{\Omega_{ij}} \quad (1)$$

where

$$\mathcal{D}_{ji} = \mathcal{D}_{ij} \quad (2)$$

and

$$\mathcal{D}_{ii} \neq 0 \quad (3)$$

which is the self-diffusion coefficient.

#### Effective Diffusion Coefficient

The effective, or average, diffusion coefficients are used extensively and defined<sup>3</sup> as

$$\frac{(1-x_i)}{D_{im}} = \sum_{j \neq i} \frac{x_j}{\mathcal{D}_{ij}} \quad (4)$$

These coefficients are defined values in the detailed and Stefan-Maxwell equations, but are used in the approximate equations as the diffusion of species "i" in the mixture as an average for the other species. Additional comments on the average diffusion coefficients are given in the discussion on the approximate diffusion equations.

#### Detailed Multi-Component Diffusion

The detailed equation<sup>1,2</sup> for the diffusion mass fluxes in a multi-component gaseous mixture is given by

$$J_i = \frac{\rho M_i}{M^2} \sum_{j \neq i} M_j \mathcal{D}_{ij} \nabla x_j \quad (5)$$

where the multi-component diffusion coefficients are given by

$$D_{ij} = \frac{M}{M_j} \frac{\left( |F^{ji}| - |F^{ii}| \right)}{|F|} \quad (6)$$

where  $|F|$  is the determinant of the elements of  $F_{ij}$  given by

$$F_{ij} = \frac{x_i}{\mathcal{D}_{ij}} + \frac{M_j}{M_i} \frac{(1-x_i)}{D_{im}} \quad \text{for } j \neq i$$

and

$$F_{ij} = 0 \quad \text{for } j = i \quad (7)$$

and  $F^{ji}$  are the transposed, co-factors of the matrix  $F$ . Unlike binary diffusion coefficients,

$$D_{ji} \neq D_{ij} \quad (8)$$

and

$$D_{ii} = 0 \quad (9)$$

The diffusion mass fluxes given by Eq. 5 are sufficient for a solution, and no other closure equation is required to ensure the mass fluxes sum to zero as required by mass conservation.

In the present study, the equations are solved in a straightforward manner. The main determinant and the co-factor determinants are solved in a standard determinant routine. There are  $(n^2 + 1)$  determinants to be solved, where “ $n$ ” is the number of species in the gas mixture. There is one main determinant of size  $(n \times n)$  and  $n^2$  co-factor determinants of size  $(n - 1) \times (n - 1)$  each. Thus as the number of species is increased, the number and the size of the determinants increases rapidly.

For a ternary mixture, analytical equations<sup>2</sup> have been derived from the determinant solutions. The diffusion coefficients are given by

$$D_{ij} = \mathcal{D}_{ij} \left[ 1 + \frac{x_k \left( \frac{M_k}{M_j} \mathcal{D}_{ik} - \mathcal{D}_{ij} \right)}{x_i \mathcal{D}_{jk} + x_j \mathcal{D}_{ik} + x_k \mathcal{D}_{ij}} \right] \quad (10)$$

where the six coefficients are calculated by rolling the  $i, j, k$  indices from 1 to 3, and the three diagonal coefficients,  $D_{ii}$ , are zero as given by Eq. 9.

### Stefan-Maxwell Equations

The Stefan-Maxwell equation<sup>1,3</sup>, originally developed to solve for the mole fraction gradient, can be used to solve for multi-component diffusion. It is given by

$$\nabla x_i = \frac{M}{\rho} \sum_{j \neq i} \left( \frac{x_i J_j}{M_j \mathcal{D}_{ij}} - \frac{x_j J_i}{M_i \mathcal{D}_{ij}} \right) \quad (11)$$

One can solve any combination of  $(n-1)$  equations for  $\nabla x_i$  in Eq. 11 to recover the remaining equations. Consequently, Eq. 11 is a set of  $(n - 1)$  independent

equations, and a closure equation, such as summation of the fluxes equal zero, is required to solve for the “ $n$ ” derivatives.

In the present study, the Stefan-Maxwell equations are re-arranged and solved for “ $J_i$ ” for equation sets in terms of mole fraction gradient and mass fraction gradient. In terms of mole gradient the equations are given by

$$J_i = -\rho \frac{M_i}{M} \frac{D_{im}}{(1-x_i)} \nabla x_i + \frac{c_i}{(1-x_i)} D_{im} \sum_{j \neq i} \frac{M J_j}{M_j \mathcal{D}_{ij}} \quad (12)$$

or also by

$$J_i = -\rho \frac{M_i}{M} \left( \frac{1-c_i}{1-x_i} \right) D_{im} \nabla x_i + \frac{c_i}{(1-x_i)} D_{im} \sum_{j \neq i} \left( \rho \frac{M_i}{M} \nabla x_j + \frac{M}{M_j} \frac{J_j}{\mathcal{D}_{ij}} \right) \quad (13)$$

In terms of mass fraction gradient the equations are

$$J_i = -\rho D_{im} \nabla c_i + \frac{c_i}{(1-x_i)} D_{im} \sum_{j \neq i} \left( \rho \frac{M}{M_j} \nabla c_j + \frac{M}{M_j} \frac{J_j}{\mathcal{D}_{ij}} \right) \quad (14)$$

Equations 12 and 14 are actually used to calculate the mass fluxes, whereas Eq. 13 is given for illustrative purposes.

Again, Eqs. 12–14 are each a set of  $(n - 1)$  equations, and a closure equation is required. In the present study, an iterative scheme is used for each set of equations in conjunction with a closure equation. The closure equation used in the iterative scheme is given by

$$J_i^{N+1} = J_i^N - c_i \sum J_j^N \quad (15)$$

The “ $J_i$ ” for each species in the “ $n$ ” species set is solved for by Eq. 12 or 14 at iteration “ $N$ ”, and then the entire set is corrected for iteration “ $N+1$ ” by the closure equation, Eq. 15. The process is repeated for a specified number of 10 iterations to reach convergence. The leading term of Eq. 12 or 14 is used as the first guess to start the iteration process. In this scheme the problem is over specified, solving for “ $n$ ” species rather than  $(n - 1)$  species with Eq. 12 or 14; however, it is a very effective method as discussed in the results. Also, by solving for all “ $n$ ” species rather than “ $n - 1$ ” species, this iterative scheme has the advantage of not requiring a decision of which “ $n - 1$ ” species to solve for by Eq. 12 or 14 and which remaining species to solve with a closure equation.

## Binary Diffusion

Before giving the approximate, multi-component equations, the equations for diffusion in a binary mixture<sup>2,3</sup> are presented for comparison and discussion purposes with the approximate methods.

By the use of Fick's law, binary diffusion in terms of mass fraction gradient is given by

$$J_i = -\rho \mathcal{D}_{ij} \nabla c_i \quad (16)$$

and in terms of mole fraction gradient, by

$$J_i = -\rho \frac{M_i}{M} \frac{M_j}{M} \mathcal{D}_{ij} \nabla x_i \quad (17)$$

Equation 17 is the commonly presented form, but it can also be written as

$$J_i = -\rho \frac{M_i}{M} \left( \frac{1-c_i}{1-x_i} \right) \mathcal{D}_{ij} \nabla x_i \quad (18)$$

The mass gradient and mole gradient forms are equivalent and only differ by the application of a transformation of mass fraction gradient to mole fraction gradient for a binary gas mixture.

## Approximate, Multi-Component Diffusion

Two commonly used approximate equations<sup>4</sup> for multi-component diffusion are examined in the present study, one in terms of mass fraction gradient and one for mole fraction gradient. In terms of mass fraction gradient, the approximate equation is given by

$$J_i = -\rho D_{im} \nabla c_i \quad (19)$$

and in terms of mole fraction gradient, by

$$J_i = -\rho \frac{M_i}{M} \left( \frac{1-c_i}{1-x_i} \right) D_{im} \nabla x_i \quad (20)$$

The solution for each species "i" can be solved for independently by application of the equations.

In the current work, the approximate equations (Eqs. 19 and 20) are taken from Ref. 4, which cites references for their source. These two equations and the equation for effective diffusion coefficient (Eq. 4) are listed in numerous publications. The short discussion herein will concentrate on those sources which appear to be close to being the original source and/or those sources which offer good insight into the equations. The expression for the effective, or average, diffusion coefficient (Eq. 4) appeared in the classical paper on mixture viscosity by Buddenberg and Wilke<sup>6</sup>

with a derivation given by Wilke<sup>7</sup> for the problem of the diffusion of species "i" with the other species being stagnate (low velocities). Also, the framework for the derivation of the effective diffusion coefficient is given in Ref. 3. The derivation is based on an analogy with binary diffusion and the use of the Stefan-Maxwell equation. The effective diffusion coefficient for species "i" is then derived for the case where all the other species move with the same velocity or are stationary. The implication is that the effective diffusion coefficient can then be substituted for the binary diffusion coefficient in Fick's law as given by Eqs. 16 or 18. Reference 1 states that Eq. 20 can be derived from the detailed multi-component diffusion equations for any species that is present as a trace species. The magnitude of the mole or mass fraction for classification as a trace species is not given. Furthermore, the article goes on to say that the equation indicates roughly that the reciprocal of the average diffusion coefficient for a multi-component mixture should be taken as the molar average of the reciprocals of the binary diffusion coefficients. In other words, Eq. 4 should be a good representation for an average diffusion coefficient. Reference 8 provides additional information along the lines presented here.

Thus, the literature suggests that the approximate equations should be adequate approximations for trace species, small mole or mass fractions, and for species with large velocities compared to the other species. The bounds on these conditions are not really defined. In many studies when one uses the approximate equations, the equations are used for all the species in the mixture and for all cases considered.

The use of the approximate equations, Eqs. 4, 19, and 20, basically states that the diffusion of a species "i" is treated such that the species "i" is one component and the other component is an average of the remaining species in a binary type of analysis. Thus, the approximate equations for diffusion are the same as the binary diffusion equations with the binary diffusion coefficient replaced with the effective diffusion coefficient. If one examines the detailed equations, see Eq. 7, or the Stefan-Maxwell equations, Eqs. 12–14, one sees that the effective diffusion coefficient is a prominent term. Also, approximate Eqs. 19 and 20 are the same as the leading terms in the Stefan-Maxwell Eqs. 14 and 13, respectively. Thus it would appear that the accuracy of the approximate equations would depend on the degree in which the last terms in Eqs. 13 and 14 approach zero. Furthermore, in the Stefan-Maxwell equations, Eqs. 12–14, if binary diffusion, Eqs. 16 and 18, is assumed for the " $J_i$ " term in the

summation, then the equations will collapse to the approximate equations. This implies that the last terms are a measure of how well the multi-component mixture deviates from a pseudo-binary mixture. Thus there is some reasonable arguments that the approximate equations have a reasonably correct form. The approximate equations will collapse to the respective binary forms for a binary gas mixture. Actually, all the equations presented will collapse to the respective binary form for a binary gas mixture.

There are some obvious problems with the approximate equations. The two forms of the equation in terms of mass fraction gradient, Eq. 19, and mole fraction gradient, Eq. 20, do not have the correct transformation between mass and mole fraction gradient for a multi-component mixture. The transformation is only correct for a binary mixture. It is possible in a multi-component mixture, except binary, for a species to have a change of sign between mass and mole fraction gradient. If this happens, then the mass and mole gradient forms of the approximate diffusion equations would give a different sign for the mass flux. Finally, the requirement of the diffusion mass fluxes summing to zero is not guaranteed.

A “corrected” form for the two approximate equations is also examined in the present study to solve the problem of the diffusion mass fluxes not summing to zero. The closure equation, Eq. 15, from the Stefan-Maxwell iterative scheme is applied to the diffusion mass fluxes to ensure the mass fluxes sum to zero by distributing the residual according to the species mass fraction. The diffusion mass fluxes are calculated independently by Eq. 19 or 20, and then corrected by

$$J_{i,corrected} = J_i - c_i \sum J_j \quad (21)$$

Thus, there are 4 basic approximate relations used in the study: Eq. 19 and 20, and the corrected form of each according to Eq. 21.

### Part I Methodology

In Part I of the present study, an examination of the equations is performed in a fundamental way. The necessary input parameters of number of species, selection of species and their properties, mole fractions, and mole fraction gradients are specified for a case, and then calculations made of the species diffusion mass fluxes. The diffusion mass fluxes for each case are calculated for detailed multi-component diffusion (including the analytical form for ternary mixtures), both the mass and mole fraction forms of the

Stefan-Maxwell equations, both the mole and mass fraction forms of the approximate equations, and both the mole and mass fraction forms of the corrected approximate equations for a total of 7 sets (8 for ternary mixtures) of equations. The detailed multi-component formulation is taken as the exact solution, and is used as the standard in defining errors in the diffusion mass fluxes.

Fourteen species (He, Ne, Ar, Kr, Xe, N<sub>2</sub>, CO, O<sub>2</sub>, CO<sub>2</sub>, CH<sub>4</sub>, CF<sub>4</sub>, SF<sub>6</sub>, C<sub>2</sub>H<sub>6</sub>, and C<sub>3</sub>H<sub>8</sub>) were used in this part. Collision cross sections were taken from the data presented in Ref. 9. The number of species ( $n = 3$  to 14), the species, the mole fractions, and the mole fraction gradients for a particular case may be either directly specified or selected by use of a random number generator. All cases are for a temperature of 300 K and a pressure of one atmosphere.

### Part I Results

Thousands of cases were run in this part of the study. Due to the large number of cases and the complexity of the results, only a few examples and a synopsis of results can be presented herein.

#### Detailed Multi-Component Diffusion

The diffusion mass fluxes summed to zero for all cases without the addition of any constraints, as they should. For all cases of ternary mixtures, the multi-component diffusion coefficients and mass fluxes agreed exactly between the detailed determinant form and the analytical form, providing confidence in the accuracy of the equations and the programming and solution procedures.

#### Stefan-Maxwell Equations

For all cases, the diffusion mass fluxes calculated from both the mole and mass gradient forms of the equations agreed exactly with the results from the detailed multi-component equations. The iteration scheme was fixed at 10 iterations. Shown in Fig. 1 is typical convergence histories of the errors in diffusion mass fluxes, as compared to the final detailed results, for both the mole and mass gradient forms of the equations. As seen, the scheme converges easily in 10 iterations, where only 6 to 7 iterations were needed to converge to 5 significant figures. These results show that the presented scheme is an effective solution procedure for solving the diffusion mass fluxes with the Stefan-Maxwell equations.

### Approximate, Multi-Component Diffusion

The approximate equations were derived for the flux of a species under the assumption of it being a trace species or the other species are diffusing at a much lower velocity. In practice, the approximate equations are often used to solve for all the species mass fluxes in a given mixture. It is this practice that is primarily examined in the present study. Due to the wide difference in results for the numerous cases, it is difficult to display the results and to provide definitive conclusions for the four approximate equations as one might expect. A few examples will be presented and then some general observation of all the results given.

Three measures selected to judge the accuracy of the diffusion mass flux results from the approximate equations are the root mean square error (RMS) for all the species in a mixture, the maximum absolute error of any species in a mixture, and the absolute errors of all the species in a mixture. For these cases the inputs are randomly generated. The cumulative numbers of these errors for 1000 mixtures comprised of 10 species randomly selected are presented in Figs. 2–4. In these figures the x-axis is the error in percent and the y-axis is the cumulative number of mixtures or species with errors in the diffusion mass fluxes less than the x-axis value. Note that the cumulative number in Figs. 2 and 3 do not reach the 1000 mixtures specified because only errors up to 100% are plotted. The difference from 1000 at 100% are mixtures which had errors larger than 100%, errors in the hundreds and thousands. The same basic reason applies to the fact that the cumulative number for all the species does not reach 10000 (1000 mixtures times 10 species) in Fig. 4. The results are plotted for the approximate equations in terms of mole and mass fraction gradient and the corrected forms of these two equations. It was noted that the results for the mole and mass fraction gradient forms of the approximate equations generally bracket the detailed results. Thus, the errors for the average of the results from the mole and mass equations and the corrected form of the average are also shown.

As shown in Fig. 3, only about 60 mixtures (6%) had errors of less than 20% for all the species in a mixture for either the mole or mass fraction form, whereas the corrected forms of mole fraction gradient or average provided results of less than 20% maximum error for approximately 57% of the mixtures. Generally the error for one or two species was large; thus, one can see from the RMS error plot, Fig. 2, the cumulative numbers with RMS errors of less than 20% are much larger than for the maximum error of any one species.

Also note in Fig. 4 that 6000 out of the possible 10000 species (60%) had errors less than 20% for the uncorrected mole or mass gradient equations, and the cumulative number went to almost 9000 for the corrected mole or average form. In general, the results show that the approximate equations are not necessarily accurate for determining the mass flux for all species in a mixture. The equations do provide better accuracy if one can accept a RMS average type of error. The corrected mole fraction gradient form or the corrected average provide the more accurate results.

The results given in Figs. 2–4 are reproducible, even though the inputs were randomly selected, and typical of the volume of solutions obtained. When another 1000 mixtures of 10 species are randomly selected, the results are the same. Also, a set of 500 mixtures provides similar results. Furthermore, if one selects 1000 mixtures of randomly selected “*n*” species mixtures, the cumulative numbers are slightly different, but the basic results are the same.

The above results represent those for many solutions. Some results from particular solutions, not necessarily typical, are presented in Figs. 5–12. The results are for mixtures with perturbations from base mixtures composed of  $N_2$ ,  $CO$ ,  $O_2$ , and  $C_2H_6$  in which the molecular weights are 28 to 32 gm/mole. In these figures the x-axis gives the mole fraction of the listed species. The mole fractions of the other species are equal amounts of the remaining mole fraction. The results are from the mole fraction form of the approximate equations, except for Fig. 12. The value listed in parenthesis on the figures by the species name is the specified mole fraction gradient. In Figs. 5–9, the species listed on the x-axis has the largest value, with the other species having an opposite sign and equal values to ensure the mole fraction gradients sum to zero as required. This series of mixtures is an attempt to assess the assumption that the approximate equations are accurate for a species in a mixture in which the other species move with the same velocity or are stationary. The velocities cannot be specified, so the mole fraction gradients were specified in an attempt to accomplish basically the same effect.

In Fig. 5 the results are presented for the base mixtures in which  $N_2$  was the species selected to vary the mole fraction. As shown, the error in the diffusion mass flux for  $N_2$  is less than 2.5% for all values of the mole fraction. (For this mixture the error was reasonably small for all species.) Next the species He was added to the base mixtures and specified as the dominant species in terms of mole fraction gradient. As

shown by the results in Fig. 6, the error was less than 1% for He. However, the other species had large errors. For these mixtures  $N_2$  was then selected as the dominant species. The results are presented in Fig. 7 and show that the error for  $N_2$  is less than 7% for all mole fractions. Interestingly, the He error remained very small. Next, the He was replaced with the high molecular weight gas Xe in the base mixtures. Again, as shown in Fig. 8, the error was small for the dominant species Xe across the mole fraction range. For these mixtures Xe was then replaced by  $N_2$  as the dominant species and the results are presented in Fig. 9. As shown, the error for  $N_2$  was less than 8%. The results in Figs. 5–9 suggest that the approximate equation does provide accurate results for a species that is dominant in terms of mole fraction gradient for a wide range of mole fraction, including large mole fractions. Unfortunately, the results also seem to suggest that accurate results are possible for all the species in a mixture with small mole fractions. However, this is misleading as discussed next.

Results for the base mixtures are presented in Figs. 10–12. For these solutions  $N_2$  and CO have specified small values of mole fraction gradient of equal value but of opposite sign. The species  $O_2$  and  $C_2H_6$  have opposite signs and equal large mole fraction gradients. The mole fraction of  $N_2$  is varied from an extremely small value to approximately 1. The other three species have equal values of mole fraction. Figure 10 shows the error in the diffusion flux as a function of the mole fraction of  $N_2$ , where the actual fluxes are presented in Figs. 11 and 12 for the approximate equation, Eq. 20, and the detailed equations, Eqs. 5–7, respectively. As shown in Fig. 10 the errors for  $N_2$  are in thousands of a percent around a mole fraction of 0.1, which is a small value. The reason for the large values and rapid change in sign of the error can be found by examination of the mass fluxes presented in Figs. 11 and 12. For the approximate equation, the mass flux calculated will always be of opposite sign to the mole fraction gradient; whereas, as shown by the detail solution, the mass flux can be of either sign as compared with the sign of the mole fraction gradient. This change in sign occurred at a mole fraction of approximately 0.1. From the Stefan-Maxwell equations, Eqs. 12 and 13, it is seen that the summation terms (the influence of the actual diffusion fluxes), which are left out of the approximate equations, control the change in sign.

It cannot be easily seen in Fig. 10, but the errors for  $N_2$  approach zero at mole fractions less than 0.01 and are about 110% at mole fractions greater than 0.25. As

given in the Equations Section, Ref. 1 presented the approximate equation, Eq. 20, as being accurate for the mass flux of a trace species in a mixture. The magnitude of the mole or mass fraction was not given to define trace species. The present results have shown the approximate equation can be accurate for many cases with rather large mole fractions. However, to guarantee the approximate equation to be accurate, the mole fraction must be extremely small,  $10^{-3}$  or smaller.

Based on the results obtained in the present study, some general observations of the accuracy of the approximate equations are as follows:

1. The assumption of the equations being accurate for a trace species in a mixture appears correct provided the mole fraction is less than 0.001 to guarantee accuracy.
2. The assumption of the equations being accurate for a species in a mixture with the other species being stationary or with much lower velocities appears correct.
3. In general, good accuracy cannot be guaranteed for a species or all species in a mixture. The errors for a case and an approximate equation can vary widely between the species.
4. Small values of the mole fraction (order of 0.1) do not necessarily lead to small errors. Conversely, values of the mole fraction as large as 0.2 to 0.5 routinely had errors less than 10%.
5. The average root mean square error for a case for the four approximate equations was 20% or less for most cases.
6. The mole fraction and mass fraction gradient of a species can be of opposite sign depending on the molecular weights and fractions comprising the mixture. This sign change was routinely observed for the random selected cases. Errors in the hundreds to thousands of percent can occur when this happens.
7. The mole fraction and mass fraction gradient forms of the approximate equations cannot be consistent when the sign change occurs between the mole fraction and mass fraction gradients for a species. The equations will give answers of opposite sign. (See Eqs. 19 and 20.)
8. The results for the mole fraction and the mass fraction gradient forms of the approximate

equations generally bracket the detailed results.

9. Based on the average root mean square errors, the errors are less for the “corrected” than the uncorrected approximate equations. The “corrected” mole fraction gradient form would be the preferred choice of the four basic approximate equations.

### Binary Diffusion:

Cases were run for binary diffusion with all the equations—detailed, Stefan-Maxwell, and all the approximate. For all the binary cases, the diffusion coefficients and diffusion mass fluxes agreed exactly among all the equations as they should. Like the detailed ternary calculations, this result provides confidence in the accuracy of the programming and solution procedures.

### Part II Methodology

In this part of the study the effects of multi-component diffusion, as calculated by the various equations, are examined within flowfield solutions obtained with the LAURA<sup>5</sup> code for Earth entries. Originally, the approximate equation for mole fraction gradient, Eq. 20, was the default option in the LAURA code. The iterative scheme for the Stefan-Maxwell equation, Eq. 12, and all the approximate forms of the equations have been added to the LAURA code. The detailed multi-component equations were not added since the results of Part I showed that the Stefan-Maxwell scheme is a highly efficient method and the results agreed exactly with the detailed equations without the overhead of solving large determinants.

The LAURA code is an upwind-biased, point-implicit relaxation algorithm for obtaining the numerical solution to the Navier-Stokes equations for three-dimensional, hypersonic flows in thermochemical nonequilibrium. Detailed information on the formulation of the LAURA code is given in Refs. 5 and 10 with a current overview given in Ref. 11. The effects of the various equations are examined by a typical flowfield solution for the Earth entry of the Stardust sample return capsule which is a Discovery class mission to rendezvous with a comet and return samples of comet particles to Earth. The Stardust capsule is a spherically-blunted, 60 degree half-angle conical forebody shape with a 0.23 meter nose radius and maximum radius of 0.41 meters. Information on the configuration and aerothermodynamics is given in

Refs. 12–14. The present solutions are obtained for thermochemical nonequilibrium flow of air for an 11 species set composed of N, O, N<sub>2</sub>, O<sub>2</sub>, NO, N<sup>+</sup>, O<sup>+</sup>, N<sub>2</sub><sup>+</sup>, O<sub>2</sub><sup>+</sup>, NO<sup>+</sup>, and e<sup>-</sup>. A fully catalytic wall condition is assumed. The computations are made at an actual Stardust trajectory point near peak heating with a freestream velocity of 10.9 km/s and a freestream density of  $2.7 \times 10^{-4}$  kg/m<sup>3</sup>, and then at the same density for progressively lower velocities of 7.0 and 6.0 km/s.

### Part II Results

The effects of the multi-component diffusion model on the surface heating distribution over the forebody of the Stardust capsule are shown in Fig. 13 for the freestream velocity of 10.9 km/s. The heating rates from the solutions with the Stefan-Maxwell equation and the “corrected” approximate equations, both mole and mass gradient forms, are in excellent agreement, whereas the heating rates via the standard approximate equations are significantly different with the mass gradient form being 80% higher and the mole gradient form being 28% lower. This bracketing of the correct results by the mole and mass gradient forms of the approximate equations was noted in Part I. The solution using the Stefan-Maxwell equation is the most accurate. As a point of interest, the wide difference in the heating rates between the mole and mass gradient forms of the approximate equations noted in some early calculations at this condition is what led to the present study. Presented in Fig. 14 are the mole fraction distributions of N<sub>2</sub>, N, O<sub>2</sub>, and O through the shock layer at the stagnation point. These results are shown only for the mole gradient equations. As shown, the mole fractions are in good agreement through the shock layer for the Stefan-Maxwell equation and the “corrected” approximate equation. Again, the standard approximate equation is in least agreement. These features are most easily seen in Figs. 14(b) and (d) for the atomic species.

For a highly reactive flowfield which forms at this entry condition, the surface heat transfer is highly dependent on the recombination of species releasing the heats of formation at the wall due to species diffusion carrying energy from the high-temperature, dissociated and/or ionized outer region of the shock layer to the cooler surface. The recombination of atomic species in the 10.9 km/s case was due to recombination of N and O to N<sub>2</sub> and O<sub>2</sub>, respectively, with the energy transport being approximately 400 w/cm<sup>2</sup> for O and 200 W/cm<sup>2</sup> for N, for a total of approximately 600 W/cm<sup>2</sup> of the total stagnation-point heating rate of 1100 W/cm<sup>2</sup>.

Heating distributions from the 7.0 and 6.0 km/s solutions are presented in Figs. 15 and 16, respectively. (Note, solutions for the approximate equations with mass gradients were not done for the 6.0 km/s case.) The effects from the choice of diffusion model were the same as discussed for the 10.9 km/s case. That is, the results for the Stefan-Maxwell and the “corrected” approximate equations are in good agreement, and the standard approximate equations disagree. However, the extent of disagreement of the approximate equations was less as the freestream velocity is decreased, and the production and diffusion of dissociated and/or ionized species is less, thereby reducing the significance of recombination energy release at the wall. The disagreement in stagnation-point heating rate of the mole gradient, approximate equation with the Stefan-Maxwell equation is 28%, 15%, and 11% as the freestream velocity goes from 10.9, 7.0, to 6.0 km/s, respectively. For the 6.0 km/s case, the recombination of O is the dominate source, being approximately 70 W/cm<sup>2</sup> while the N recombination is only 5 W/cm<sup>2</sup> at the stagnation point.

The detailed multi-component equations, Eqs. 5–7, were not added to the LAURA code because of the high overhead associated with solving the large number and sizes of determinants. Also, the presented iterative scheme for solving the Stefan-Maxwell equations, Eqs. 12 and 14, was found to be an efficient and accurate method in Part I. In Part II the accuracy of the iterative scheme for the Stefan-Maxwell equations, as implemented in the LAURA code, has been assessed as follows. The required basic data from selected grid points from all three velocity cases were extracted from the converged solutions, and then calculations were made with the detailed and Stefan-Maxwell equations in the computer program used in Part I. For all comparisons, the diffusion mass fluxes from the mole and mass gradient forms of the Stefan-Maxwell equations agreed exactly with the detailed equations, and these results agreed exactly with the mass fluxes from the LAURA code using the Stefan-Maxwell scheme. Also, there were no cases in which the scheme failed to converge. In LAURA, the diffusion mass fluxes from the Stefan-Maxwell method are checked to converge within 10<sup>-6</sup> between successive iterations with an upper limit of 40 iterations. Examination of the convergence history showed that less than 10 to 11 iterations were required.

In any large CFD code there are trades between storage and computational time of the fluid thermodynamic and transport properties. Also, there is the judgment of how often to update the fluid properties

between iterations of the basic flow equations. The approximate diffusion equations have the advantage that only “*n*” effective diffusion coefficients need to be saved between a specified number of flow iterations before being re-calculated from the binary diffusion coefficients and updated, whereas the Stefan-Maxwell equations require the binary diffusion coefficients to be calculated every iteration or “*n*(*n* – 1)/2” binary diffusion coefficients stored between updates. Thus, the approximate equations have an advantage in storage requirements and computational time. The “corrected” approximate equations retain this advantage. In the LAURA code, the approximate equations, uncorrected and corrected, are calculated from the effective diffusion coefficients which are updated with calculations of the binary diffusion coefficients every 10 to 20 iterations. When the Stefan-Maxwell scheme is used, the solution is converged, or nearly so, using the “corrected” approximate, mole gradient, method for the diffusion fluxes and then switched over to the Stefan-Maxwell equations in which the binary diffusion coefficients are calculated every iteration until final convergence. In general, the Stefan-Maxwell method requires approximately 50% more time per iteration than the approximate equations, with a total time increase of approximately 10% for a converged solution by the overall method given above.

### Concluding Remarks

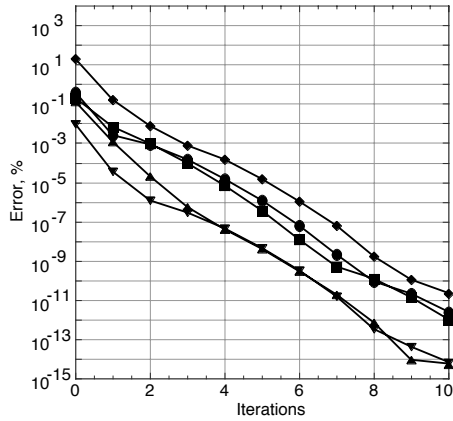
The accuracy and complexity of calculating multi-component gaseous diffusion with the detailed equations, the Stefan-Maxwell equations, and approximate equations have been examined in a basic study in which the inputs are specified, and in applications with the Langley Aerothermodynamic Upwind Relaxation Algorithm (LAURA) code for Earth entry of a high-velocity spacecraft. The iterative scheme presented for the Stefan-Maxwell equations is determined to be an efficient method and as accurate as the detailed equations. This method is highly recommended for applications in computational fluid dynamics codes.

In general, the approximate equations provided inaccurate solutions, and are of questionable usage for calculating the diffusion mass fluxes of all the species or even a single species in a mixture. However, for the assumed conditions for which the approximate equations were derived, it appears the approximate equations may be valid, that is, for a trace species in a mixture, or for a species in which the other species in the mixture are stationary (low velocity). The

definition as a trace species may require the mole fraction to be less than approximately 0.001 to guarantee accurate results. The “corrected” forms of the approximate equations that ensure the diffusion mass fluxes sum to zero were significantly more accurate than the uncorrected forms; however, good accuracy was not obtained for all cases in the basic study. For the three Earth entry cases used in the applications with the LAURA code, the results with the “corrected” approximate equations were in excellent agreement with those with the Stefan-Maxwell method. Thus, based on this limited number of cases, it appears the “corrected” approximate equations may be adequate for Earth entry applications. Furthermore, the implementation of the Stefan-Maxwell scheme in the LAURA code makes use of the “corrected” equations to approach convergence of a solution before switching to the Stefan-Maxwell scheme and final convergence.

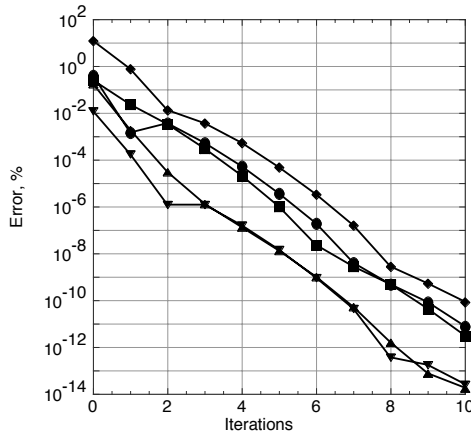
#### References

1. Curtiss, C.F. and Hirschfelder, J.O., “Transport Properties of Multicomponent Gas Mixtures,” *The Journal of Chemical Physics*, Vol. 17, No. 6, June 1949, pp. 550–555.
2. Hirschfelder, J.O., Curtiss, C.F., and Bird, R.B., *Molecular Theory of Gases and Liquids*, John Wiley & Sons, Inc., 1954.
3. Bird, R. B., Stewart, W.E., and Lightfoot, E.D., *Transport Phenomena*, John Wiley & Sons, Inc., 1960.
4. Gupta, R.N., Lee, Kam-Pui, Thompson, R.A., and Yos, J.M., “Calculations and Curve Fits of Thermodynamic and Transport Properties for Equilibrium Air to 30 000 K,” RP 1260, NASA, October 1991.
5. Gnoffo, P.A., Gupta, R.N., and Shinn, J.L., “Conservation Equations and Physical Models for Hypersonic Air Flows in Thermal and Chemical Non-equilibrium,” TP 2867, NASA, February 1989.
6. Buddenberg, J.W. and Wilke, C.R., “Calculation of Gas Mixture Viscosities,” *Industrial and Engineering Chemistry*, Vol. 41, No. 7, July 1949, pp. 1345–1347.
7. Wilke, C.R., “Diffusional Properties of Multicomponent Gases,” *Chemical Engineering Progress*, Vol. 46, No. 2, February 1950, pp. 95–104.
8. Rasmussen, Maurice, *Hypersonic Flow*, John Wiley & Sons, Inc., 1994.
9. Kestin, J., and Wakeham, W.A., *Transport Properties Of Fluids: Thermal Conductivity, Viscosity, and Diffusion Coefficient*, Hemisphere Publishing Corp., 1988.
10. Cheatwood, F.M., and Gnoffo, P.A., “User’s Manual for the Langley Aerothermodynamic Upwind Relaxation Algorithm (LAURA),” TM 4674, NASA, April 1996.
11. Gnoffo, Peter A., Weilmuenster, K. James, Hamilton, H. Harris II, Olynick, David R., and Venkatapathy, Ethiraj, “Computational Aerothermodynamic Design Issues for Hypersonic Vehicles,” AIAA 97-2473, AIAA, June 1997.
12. Mitcheltree, R.A., Wilmoth, R.G., Cheatwood, F.M., Brauckmann, G.J., and Greene, F.A., “Aerodynamics of Stardust Sample Return Capsule,” AIAA 97-2304, AIAA, June 1997.
13. Olynick, David R., Chen, Y.K., and Tauber, Michael E., “Forebody TPS Sizing with Radiation and Ablation for the Stardust Sample Return Capsule,” AIAA 97-2474, AIAA, June 1997.
14. Olynick, David R., “Aerothermodynamics of the Stardust Sample Return Capsule,” AIAA 98-0167, AIAA, January 1998.



a) Mole fraction gradient formulation

Fig. 1 Typical convergence of Stefan-Maxwell equations. Absolute error shown for 5 species mixture.



b) Mass fraction gradient formulation  
Fig. 1 Continued.

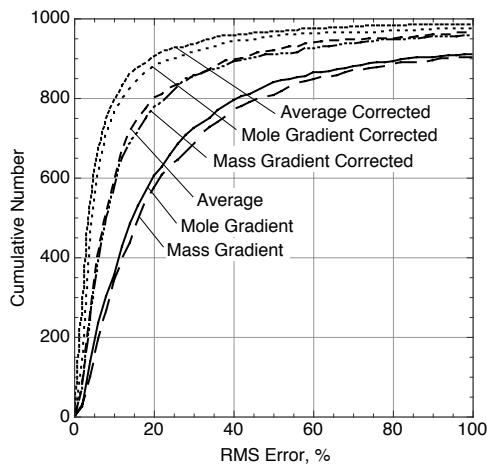


Fig. 2 Cumulative number of the root mean square (RMS) errors from the approximate equations for 1000 mixtures of 10 species.

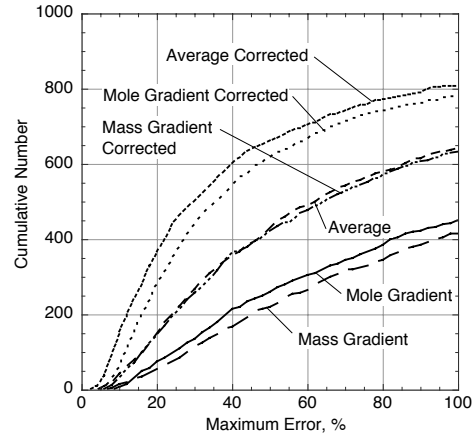


Fig. 3 Cumulative number of the maximum absolute errors from the approximate equations for 1000 mixtures of 10 species.

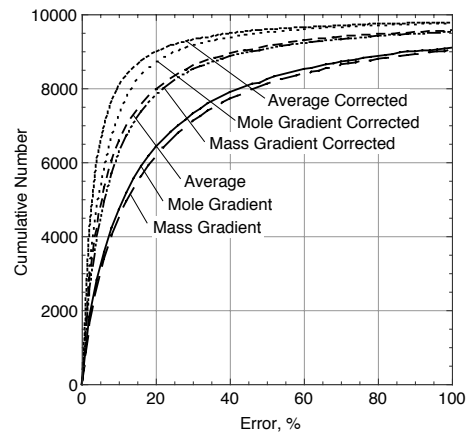


Fig. 4 Cumulative number of all the absolute errors from the approximate equations for 1000 mixtures of 10 species.

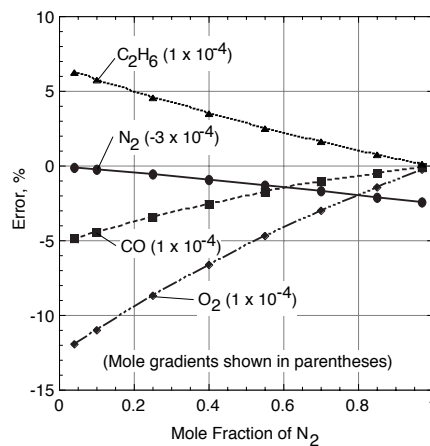


Fig. 5 Errors from approximate, mole gradient equation for base mixtures. Dominant species is  $N_2$ .

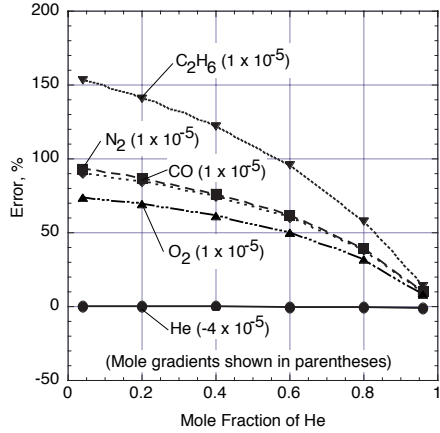


Fig. 6 Errors from approximate, mole gradient equation for base mixtures with He. Dominant species is He.

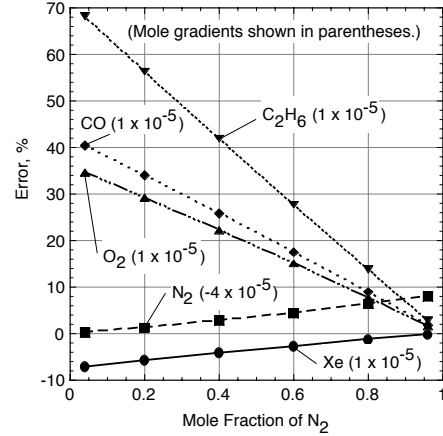


Fig. 9 Errors from approximate, mole gradient equation for base mixtures with Xe. Dominant species is  $N_2$ .

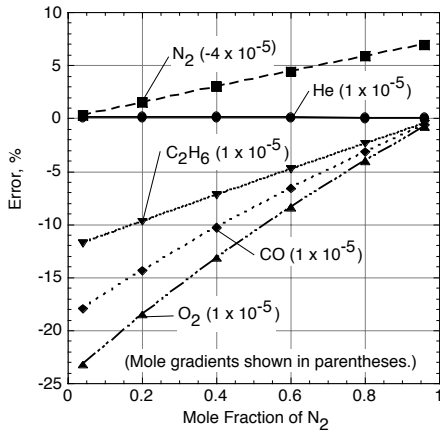


Fig. 7 Errors from approximate, mole gradient equation for base mixtures with He. Dominant species is  $N_2$ .

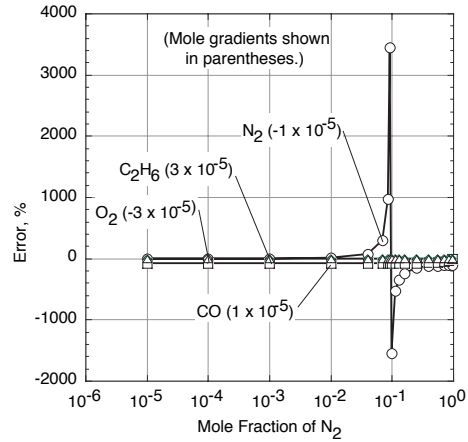


Fig. 10 Errors from approximate, mole gradient equation for base mixtures with split, equal mole gradients.

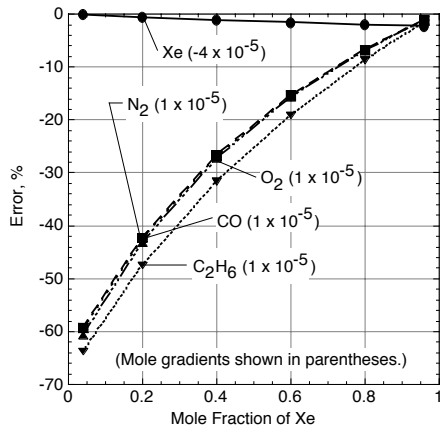


Fig. 8 Errors from approximate, mole gradient equation for base mixtures with Xe. Dominant species is Xe.

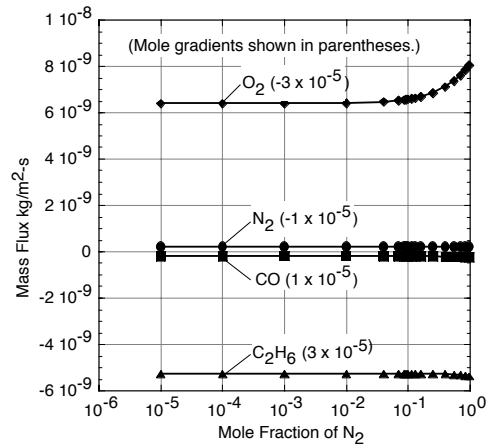


Fig. 11 Mass fluxes from approximate, mole fraction equation for base mixtures with split, equal mole gradients.

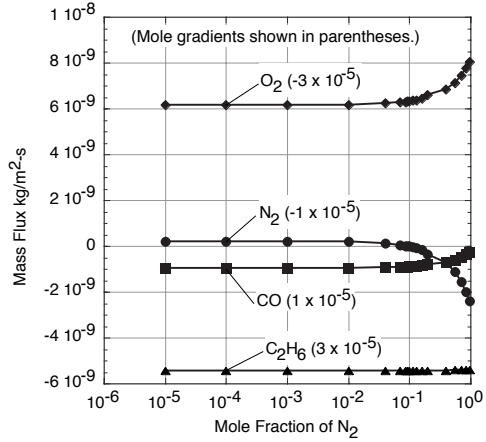
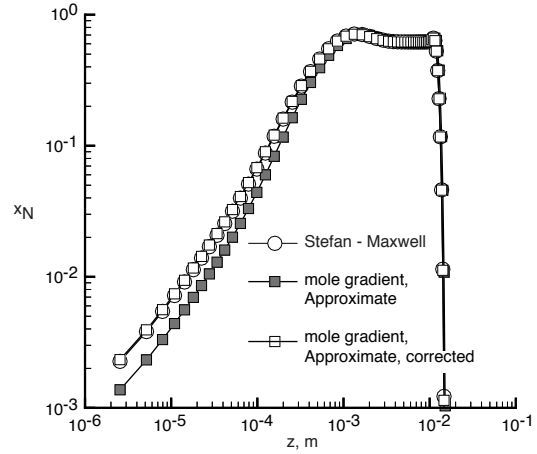


Fig. 12 Mass fluxes from detailed equations for base mixtures with split, equal mole gradients.



(b) Atomic nitrogen

Fig. 14 Continued.

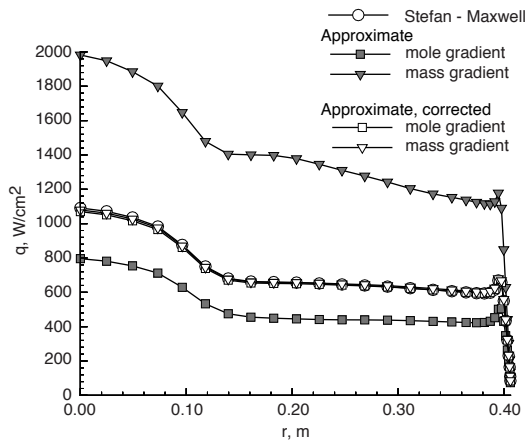
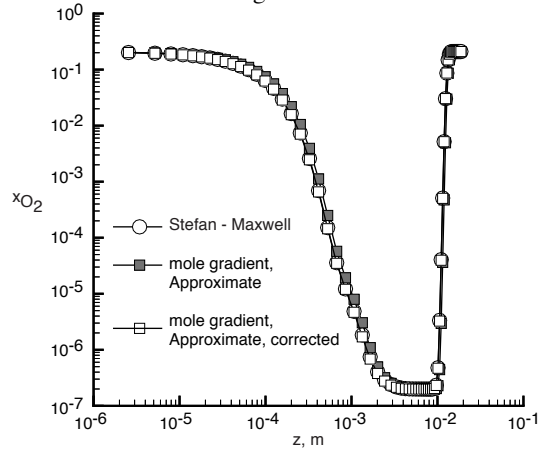
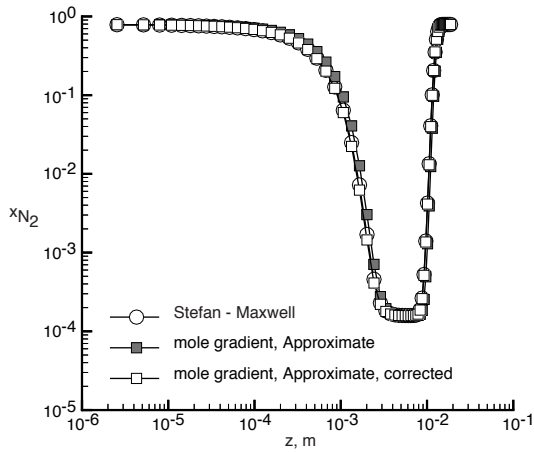


Fig. 13 Effect of diffusion model on surface heating distribution at freestream velocity of 10.9 km/s.

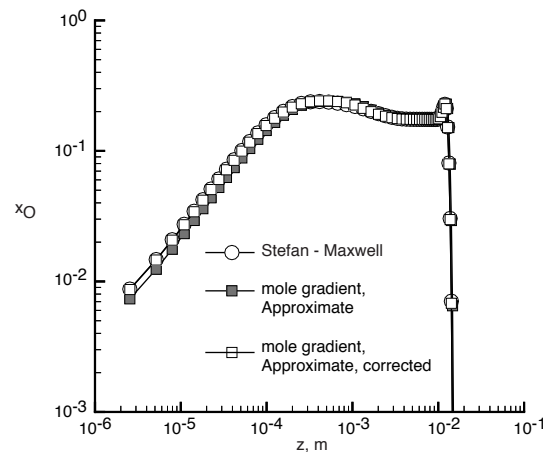


(c) Diatomic oxygen

Fig. 14 Continued.



(a) Diatomic nitrogen



(d) Atomic oxygen

Fig. 14 Concluded.

Fig. 14 Effect of diffusion model on species mole fraction distribution through shock layer at stagnation point for freestream velocity of 10.9 km/s.

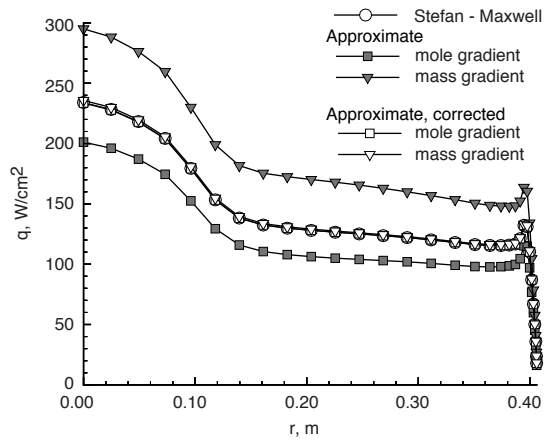


Fig. 15 Effect of diffusion model on surface heating  $q_1$  distribution at freestream velocity of 7.0 km/s.

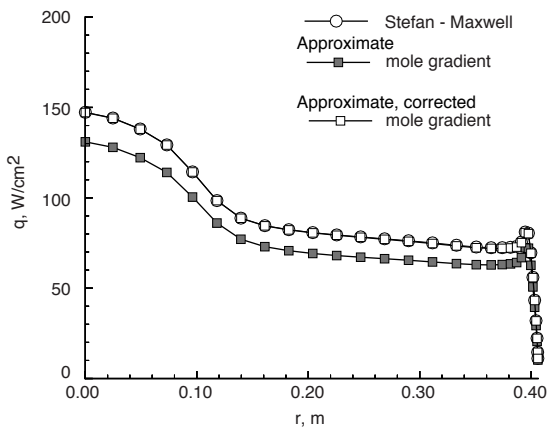


Fig. 16 Effect of diffusion model on surface heating  $q_1$  distribution at freestream velocity of 6.0 km/s.